JOURNAL OF MATERIALS SCIENCE 16 (1981) 1654–1660

Scanning electron microscopy studies of abraded rubber surfaces

ANIL K. BHOWMICK, SANJAY BASU, SADHAN K. DE
Department of Chemistry and Materials Science Centre, Indian Institute of Technology, Kharagpur 721302, India

The surfaces of polybutadiene rubber (BR) and styrene-butadiene rubber (SBR) subjected to different degrees of abrasion have been studied by scanning electron microscopy (SEM). In the case of SBR it has been shown that abrasion begins with marks in the direction of rotation which are followed by fine ribbing and then by the formation of coarse, angular and prominent ridges. Prolonged abrasion produces folding and cavities on the surface. This change in abrasion mechanism has been explained as a result of heat build-up and high crack growth rate in SBR which occur beyond a certain stage. These help in softening the matrix and removing the surface. On the other hand, fractured surfaces of BR show that ridges begin to form at about 250 revolutions and there is no characteristic difference between the abraded surfaces at lower or higher degrees of abrasion.

1. Introduction

Improvement of the abrasion resistance of vulcanized rubber is still one of the problems of the rubber industry and it is particularly important in the tyre industry. In earlier communications [1–3] it has been observed that the abrasion resistance of rubbers is not solely determined by the network structure. For example, it has been shown [2] that abrasion resistance of polybutadiene rubber (BR) is superior to styrene-butadiene rubber (SBR), although the crosslink structure does not predict such a wide variation in abrasion resistance. The abrasion of rubber is a complex process. Any measure to improve the abrasion resistance of rubber products can not be brought about without studying the mechanism of wear of rubber. Although this subject has been extensively studied over the years [4–9], the basic mechanism is still obscure. It has been shown earlier [10, 11] by scanning electron microscope (SEM) studies that the mechanism of abrasion is different from other failure mechanisms of rubber, such as tensile stress, tear and fatigue. In this paper, the abrasion of polybutadiene and styrene-butadiene rubbers subjected to different degrees of abrasion has been studied using the scanning electron microscope. An attempt has been made to explain the fractured surfaces on the basis of the increase of heat build-up and the growth rates of cracks with flexing time.

2. Experimental procedure

Table I gives the compositions of the compounds studied with optimum cure times. The details of

TABLE I Compositions of the compounds used by weight

Compound	Composition	
	Rubber (g)	Filler (g)
BR-1203*	100	–
SBR-1712†	–	100
Zinc oxide	5	5
Stearic acid	2	2
HAF Black (N-330)	50	50
Oil	6	–
Sulfur	0.5	0.5
Sulfason-R‡	1.0	1.0
CBS§	2.0	2.0
Optimum cure time (min)	14.5	18.2

*Polybutadiene rubber supplied by Indian Petrochemicals Ltd, Baroda.
†Styrene-butadiene rubber obtained from Synthetic and Chemicals Ltd, Bareilley.
‡Dithiodimorpholine obtained from Monsanto Co., USA.
§N-cyclohexyl benzothiazyl sulphenamide supplied by Alkali and Chemicals Corporation Ltd, Rishra.

0022–2461/81/061654–07$02.70/0

TABLE II Properties of the compounds and their chemical characterization

Property	SBR	BR
Tensile strength (MPa)	20.60	19.11
Tear strength ($\times 10^3$ kN m^{-1})	4.80	4.80
Elongation at break (%)	870	430
Hardness (Shore A)	51	66
Volume fraction of rubber (V_r)	0.198	0.255
Polysulfidic crosslinks (%)	40.4	31.8

the preparation of the vulcanized compounds were described in a previous publication [12]. The compound was vulcanized at 150° C. The abrasion test was carried out in a Croydon-Akron Abrader (BS 903, Pt 49: 1957 method C). A Goodrich flexometer and a De Mattia flexing machine were used to measure the heat build-up and flexing characteristics, respectively.

The tested specimens were coated with copper using a vacuum technique and the coated fracture surfaces were studied using SEM model ISI-60. SEM photographs of the tested specimens were taken within 48 h of testing. The orientation of the photographs was kept constant throughout the study.

Characterization of the compounds is reported in Table II.

3. Results and discussion

3.1. Styrene-butadiene rubber

SEM photographs of the abraded surfaces of SBR are shown in Fig. 1a to o.

It was observed that abrasion began in the direction of rotation at 100 revolutions (Fig. 1a) and there is fine, close, parallel ribbing (Fig. 1b). These abrasion patterns are at right angles to the relative motion of the rubber and abrasive. At higher revolutions (250), deep grooves are observed (Fig. 1c). The beginning of folding is shown in Fig. 1d. Fig. 1e shows a broad view of the material flow. Initiation of ribbing across the flow of the material is shown in Fig. 1f. At 500 revolutions the grooves become smoother (Fig. 1g) probably due to the loss of some material from the surface. The amount of ribbing increases (Fig. 1h) and becomes more prominent as well. Fig. 1i shows the ribs and the flow lines across each other. It is shown that the old ridges are coarse and make angles with the grain and so are removed, but the new ridges are formed parallel to the edge of the specimen (Fig. 1j). At about 1000 revolutions, a change in the mechanism of abrasion occurs. Folding on the surface of the rib takes place (Fig. 1k and l). Longitudinal ridges with fine flow lines and cavities are observed in Fig. 1m. Very coarse ribbing also becomes visible (Fig. 1n). At 1500 revolutions coarser ribbing has been observed and these ribs are mainly aligned with the edge. They are then removed from the surface. The surface between the ribs shows a rounded texture (Fig. 1o).

3.2. Polybutadiene rubber

Abraded surfaces of BR are shown in Fig. 2.

At 100 revolutions initiation of abrasion is observed and there is no sign of ridge formation (Fig. 2a). A more detailed view has been shown in Fig. 2b. The beginning of the ridge formation occurs at 250 revolutions. Ridges are very close as compared to those of SBR. Abrasion patterns are visible in Fig. 2c. At 500 revolutions, the same wavy ridges are observed as in Fig. 1b. They have a tendency to become parallel with the edge. There is no characteristic difference between the abraded surface at 500 revolutions and at 1000 revolutions. Fig. 2d shows the details of the ridge and the matrix at 1500 revolutions. The abraded surface at 1500 revolutions also shows a similar pattern. One such ridge is given in Fig. 2e. Unlike SBR, there is no sweeping action or folding.

In the following paragraphs an attempt is made to explain the fractographs of abraded surfaces on the basis of some technical properties.

Fig. 3 shows the plot of wear against number of revolutions. At lower revolutions abrasion loss of SBR is less than that of BR; at higher revolutions, the loss is greater. A similar trend is observed in the crack growth plot in Fig. 4. Heat build-up in SBR is always higher than in BR and the difference increases at longer flexing times (Fig. 5). In abrasion, heat build-up and crack resistance seem to be important. It is these two factors which are responsible for the poorer abrasion resistance of SBR at higher revolutions and the increased coarse ridging and folds on the abraded surfaces.

At lower revolutions, fractographs of the two rubbers are similar. This is evident from Figs 1b and 2c. At lower revolutions the crack resistance and the heat build-up of the two rubbers are similar.

Our results (Table II) show that tensile deformation and tear resistance as measured by ASTM methods [13] (rate of separation of the grips,

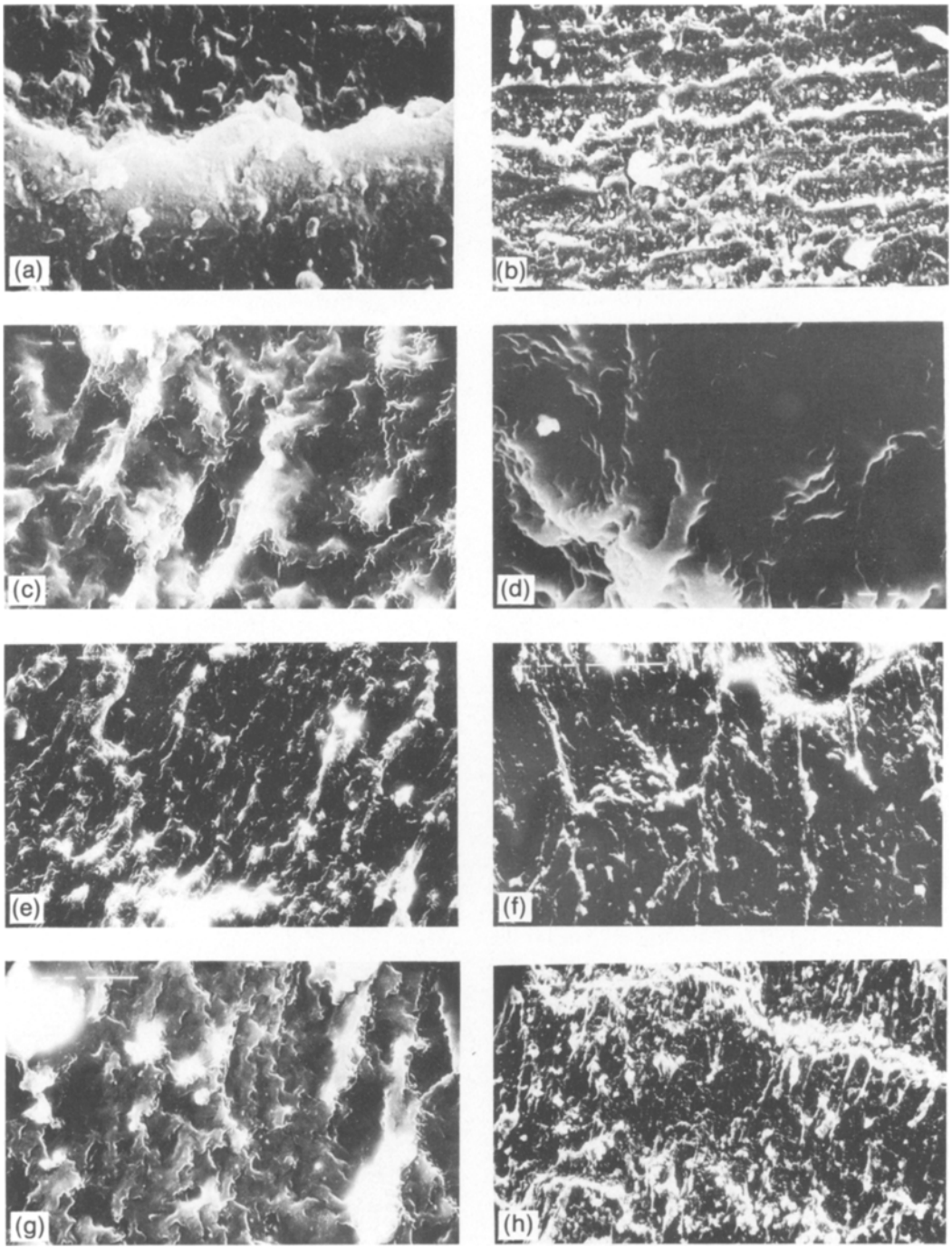

Figure 1 SEM photographs of abraded surface of SBR: (a) Secondary electron image (× 2870) showing the abrasion pattern at 100 revolutions, (b) fine parallel ribbing at 100 revolutions (× 250), (c) abrasion marks and deep grooves at 250 revolutions (× 830), (d) beginning of the folds at 250 revolutions (× 2870), (e) broad view of the materials flow at 250 revolutions (× 250), (f) initiation of ribbing across the flow line at 250 revolutions (× 124), (g) cracks and flow lines; smoother grooves at 500 revolutions (× 820), (h) ribs on the surface at 500 revolutions (× 124), (i) ribs and flow lines touching each other at 500 revolutions (× 290), (j) coarse ribbing at 500 revolutions (× 51), (k) folds on the surface of the rib at 1000 revolutions (× 2870), (l) broad view of the folds at 1000 revolutions (× 290), (m) longitudinal ridges with fine flow lines and cavities at 1000 revolutions (× 820), (n) coarse ridging at 1000 revolutions (× 40) and (o) general surface having rounded texture between the ribs at 1500 revolutions (× 820).

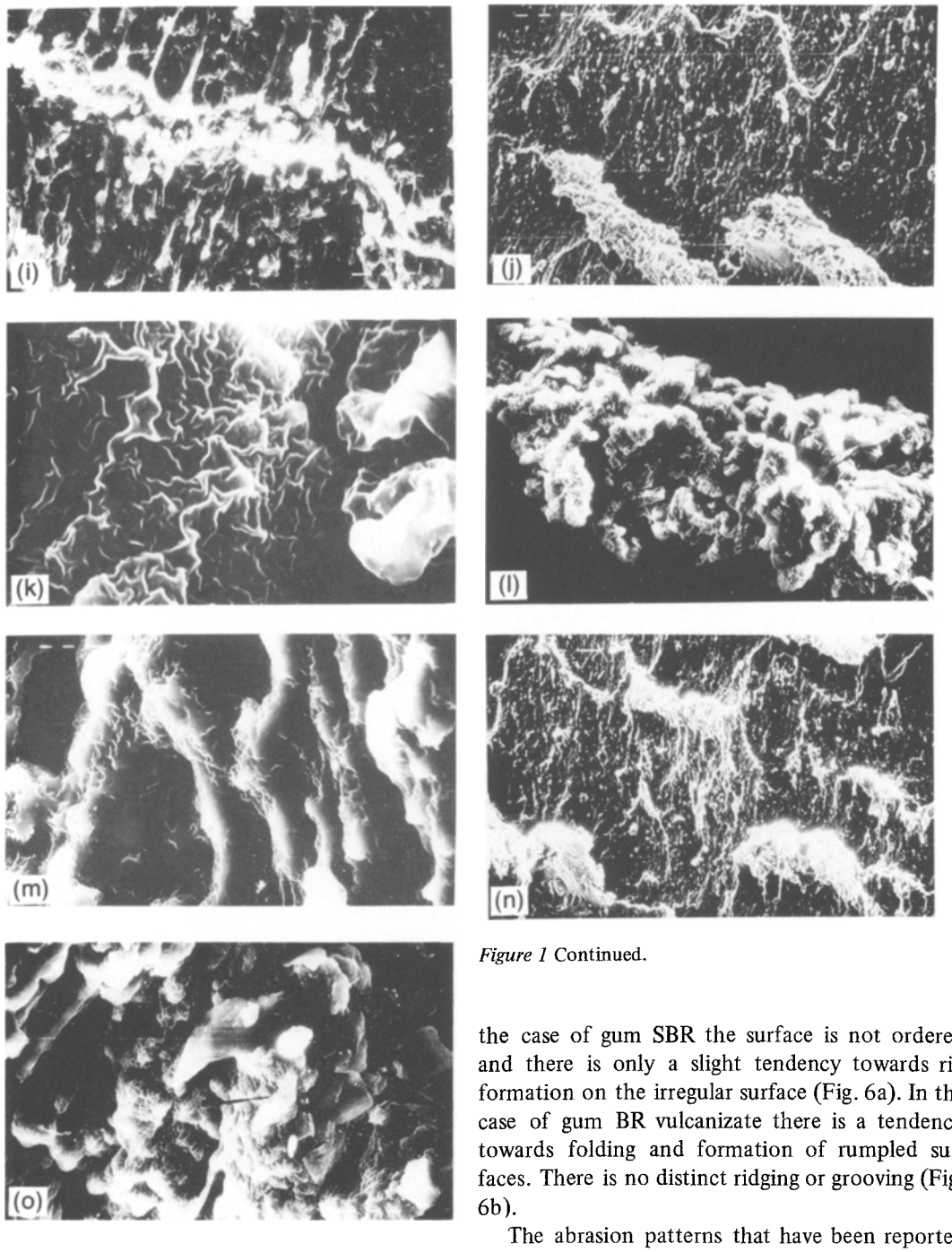

Figure 1 Continued.

20 inch min^{-1}) may not be important in abrasion. Moreover, the role of changes in network structure in abrasion has not been fully evaluated. The discussion was based on filled vulcanized material. Like tensile and tear fractured surfaces of nitrile butadiene rubber (NBR) [10], the mechanism of abrasion of gum SBR and BR vulcanizate is different from that of filled vulcanizate. For instance, in the case of gum SBR the surface is not ordered and there is only a slight tendency towards rib formation on the irregular surface (Fig. 6a). In the case of gum BR vulcanizate there is a tendency towards folding and formation of rumpled surfaces. There is no distinct ridging or grooving (Fig. 6b).

The abrasion patterns that have been reported here have been observed in earlier communications [4, 10, 11], although the abrasives in some cases are different. Even the patterns obtained from the cut of a smooth razor blade [8] are wavy ridges, as obtained in our work. It has been reported previously [11] that the abrasion of filled natural rubber vulcanizate occurs by a frictional mechanism resulting from the forces of friction created by projections which deform the surface layers and

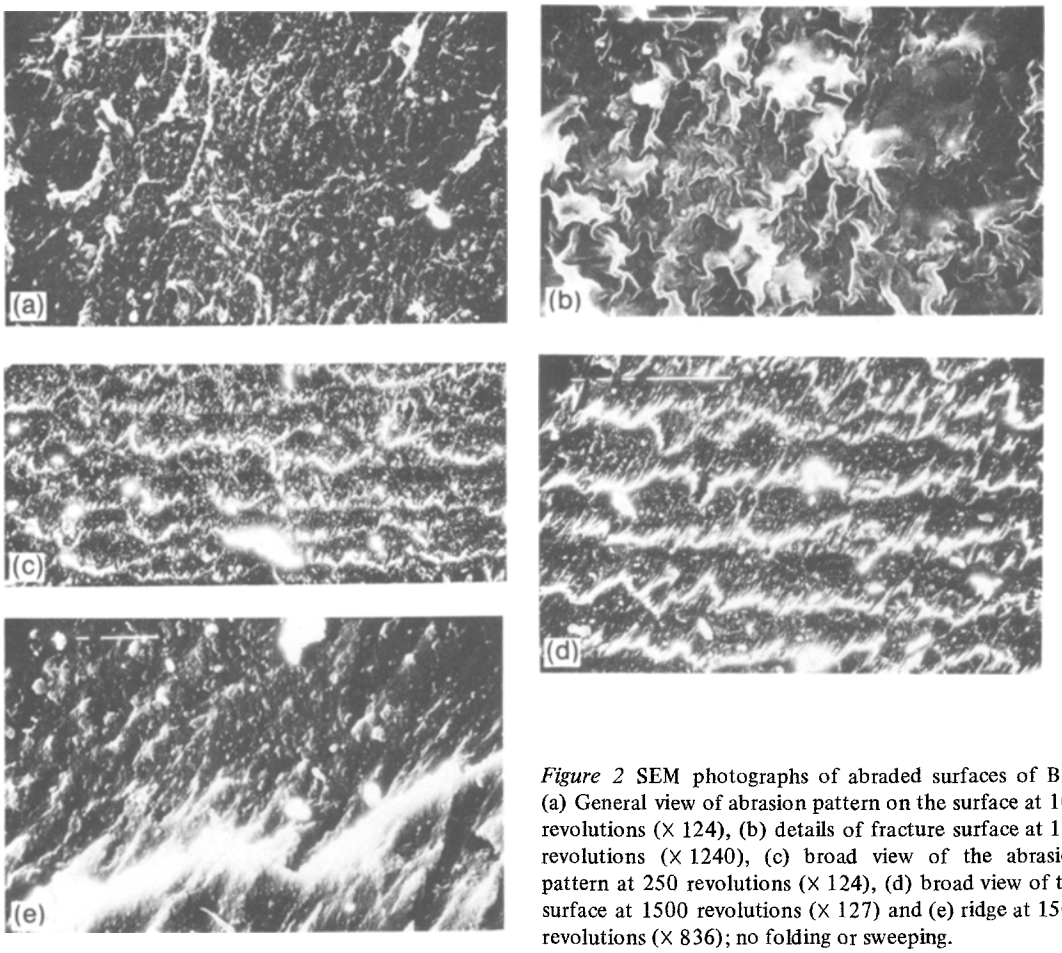

Figure 2 SEM photographs of abraded surfaces of BR: (a) General view of abrasion pattern on the surface at 100 revolutions (× 124), (b) details of fracture surface at 100 revolutions (× 1240), (c) broad view of the abrasion pattern at 250 revolutions (× 124), (d) broad view of the surface at 1500 revolutions (× 127) and (e) ridge at 1500 revolutions (× 836); no folding or sweeping.

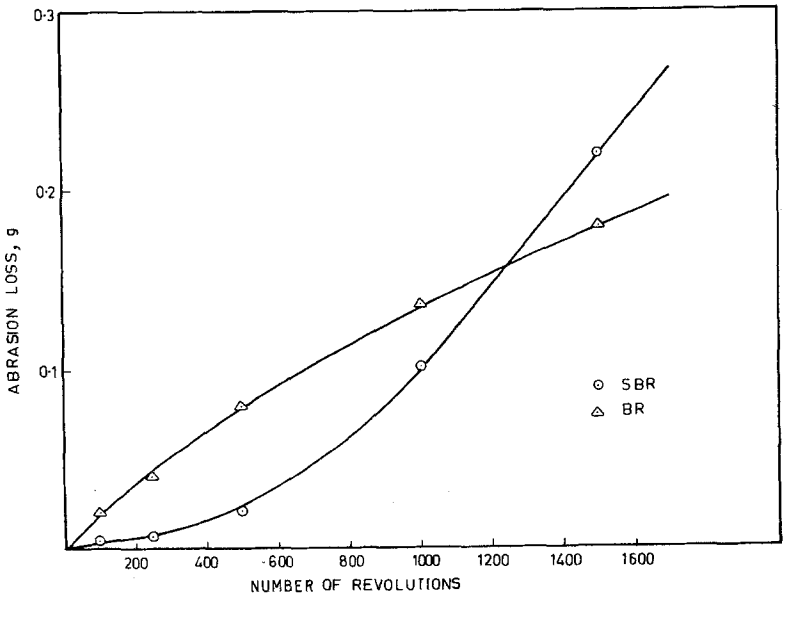

Figure 3 A plot of abrasion loss against revolutions.

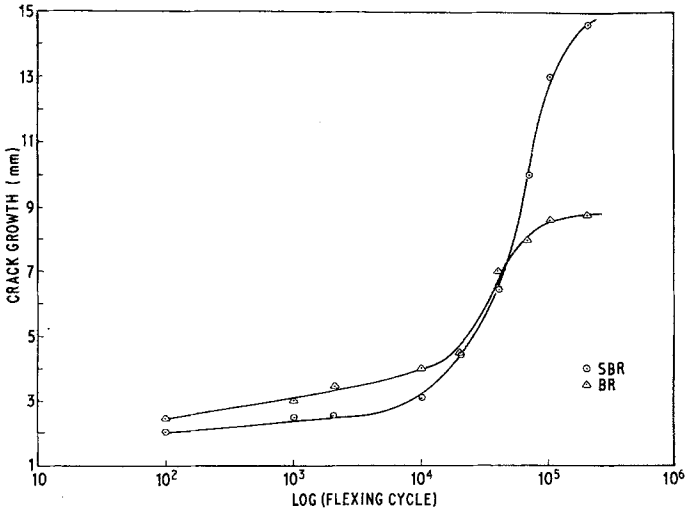

Figure 4 Plot of crack growth against flexing time.

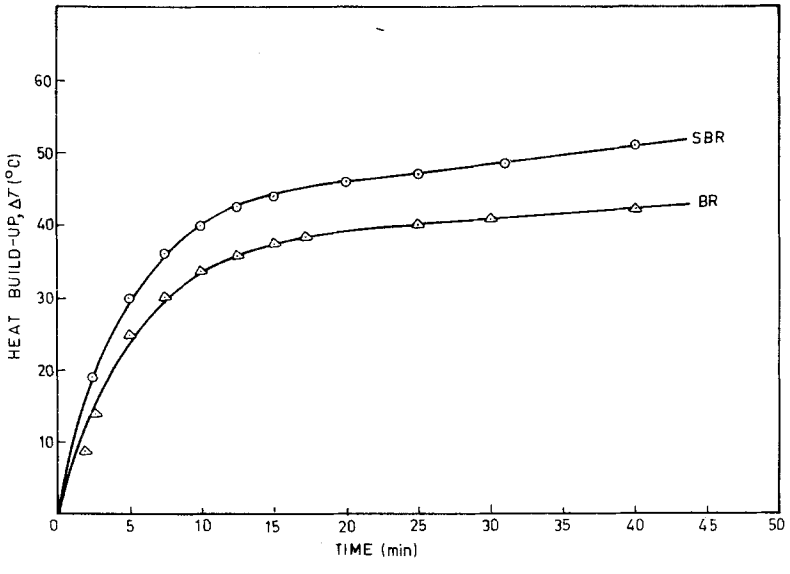

Figure 5 Plot of heat build-up against flexing time.

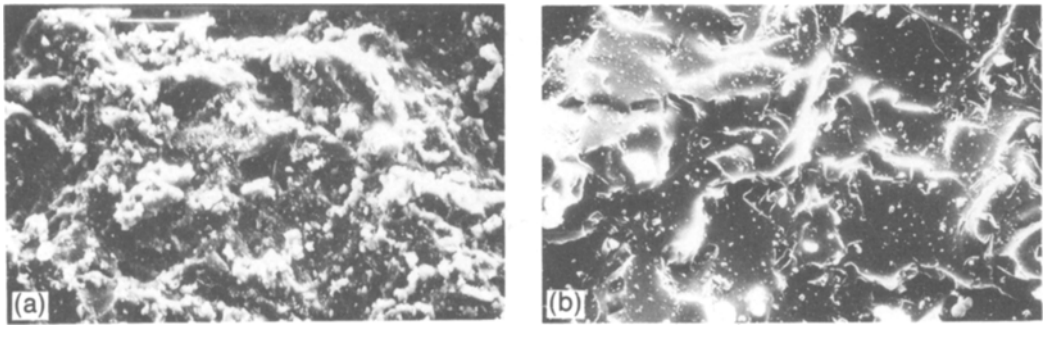

Figure 6 SEM photographs of abraded surfaces: (a) haphazard surface of gum SBR at 1000 revolutions (× 122) and (b) flecked surface of gum BR at 250 revolutions (× 287).

remove them. This mechanism is also applicable to filled SBR and BR. The gum vulcanizate follows the "abrasive" mechanism resulting from the microcutting of the surface.

Acknowledgement

Thanks are due to the Council of Scientific and Industrial Research, New Delhi, for financial assistance.

References

1. A. K. BHOWMICK and S. K. DE, *Rubber Chem. Techn.* **52** (1979) 985.
2. *Idem, J. Appl. Polymer Sci.* **25** (1980).
3. *Idem, Rubber Chem. Tech.* **53** (1980) 960.
4. D. I. JAMES (Ed.), "Abrasion of Rubber" (Maclaren and Sons Ltd, London, 1967).
5. A. SCHALLAMACH, *Wear* **1** (1958) 384.
6. K. A. GROSCH and A. SCHALLAMACH, *Rubber Chem. Techn.* **39** (1966) 287.
7. I. V. KRAGELSKII, *Soviet Rubber Techn.* **18** (1959) 20.
8. E. SOUTHERN and A. G. THOMAS, *Rubber Chem. Techn.* **52** (1979) 1008.
9. A. SCHALLAMACH, *J. Appl. Polymer Sci.* **12** (1968) 281.
10. A. K. BHOWMICK, S. BASU and S. K. DE, *Rubber Chem. Techn.* **53** (1980) 321.
11. A. K. BHOWMICK, G. B. NANDA, S. BASU and S. K. DE, *ibid.* **53** (1980) 327.
12. R. MUKHOPADHYAY, S. K. DE and S. N. CHAKRABORTY, *Polymer* **18** (1977) 1243.
13. ASTM Standards D412-51T and D624–48.

Received 2 October and accepted 5 December 1980.